



# On the interpretation of Varestraint and Transvarestraint hot cracking test results

Arne Kromm<sup>1</sup> · Maximilian Thomas<sup>1</sup> · Thomas Kannengiesser<sup>1</sup> · Jens Gibmeier<sup>2</sup>

Received: 13 November 2023 / Accepted: 30 January 2024  
© The Author(s) 2024

## Abstract

The Varestraint test and its variant Transvarestraint are one of the most widely used techniques for evaluating a material solidification cracking sensitivity during welding. The result of such tests is a crack length which is proportional to the material's cracking susceptibility. Nevertheless, the welding and load parameters can unintentionally influence the crack length, which in some cases can distort the material evaluation. An approach is described as to how these effects can be assessed with the aid of a digital crack analysis. The crack lengths are compared position-dependently with their possible propagation due to the weld pool movement during continuous loading. The index derived from this can be used by the operator to evaluate his test parameters. In addition, a comparison of the results of different Varestraint setups is made possible. Alongside experimental results, a numerical sensitivity analysis is presented on how individual welding and loading parameters can affect the crack lengths.

**Keywords** Varestraint test · Solidification cracking · Weldability · Cracks

## 1 Introduction

Solidification cracks are imperfections that can occur during the solidification of metals in fusion welding. In addition to metallurgical aspects, this type of defect is also determined by the thermomechanical boundary conditions. It is the tearing-off of liquid films on the grain boundaries due to deformations within a critical temperature range. Consequently, the solidification cracking susceptibility of a material can be described by its so-called brittle temperature range (BTR) [1]. Cracks can only occur if the augmented strains within this temperature range exceed a certain threshold.

### 1.1 Solidification cracking assessment using the Varestraint test

For assessing the susceptibility of materials to solidification cracking during welding, a variety of test methods exist [2]. One example is the Modified Varestraint Transvarestraint test (MVT) used at BAM [3], which is one of many adaptations of the Varestraint principle [4]. A specimen is subjected to a bending strain during Gas Tungsten Arc welding (GTAW), which provokes the formation of solidification cracks in the weld metal. Varestraint and Transvarestraint variants differ in terms of bending crosswise and lengthwise to the welding direction as indicated in Fig. 1. When the Varestraint test is referred to in the following, this includes all test variants, i.e., also the Transvarestraint variant.

The specimens of Varestraint tests are evaluated by quantifying the cracks formed on the specimen surface. The exact procedure is not standardized but usually requires the use of light microscopes with a fixed magnification. The result of the Varestraint test is often the so-called total crack length, which is calculated as the sum of the lengths of all cracks on the specimen surface ("total crack length," TCL). In some cases, the maximum crack length (MCL) is also given.

Besides the augmented strain-heat input, weld travel speed and deformation rate represent the decisive parameters

---

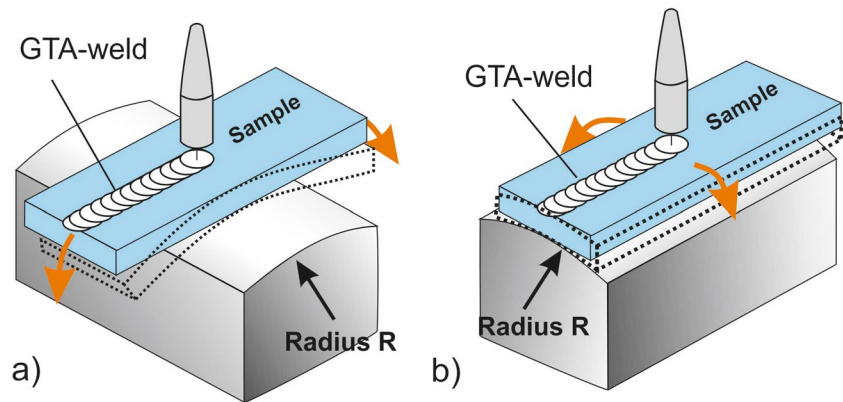
Recommended for publication by Commission II - Arc Welding and Filler Metals

✉ Arne Kromm  
arne.kromm@bam.de

<sup>1</sup> Bundesanstalt für Materialforschung und -prüfung (BAM), Berlin, Germany

<sup>2</sup> Institute for Applied Materials (IAM-WK), Karlsruhe Institute of Technology (KIT), Karlsruhe, Germany

**Fig. 1** Principle of Modified Varestraint Transvarestraint (MVT) Test, Varestraint (a) and Transvarestraint (b)



of Varestraint testing [4, 5]. There is not always an agreement in the literature about their respective influence on crack initiation, and the selection and evaluation of suitable parameters are still the subject of research [6]. Thomas et al. [7] provided a compilation of common parameter sets taken from technical standards, important publications, and selected recent studies.

Differences in the designs of the Varestraint testing machines, as well as the non-existing standardization of test parameters and procedures, make it difficult to compare results. Round robin tests have been carried out in the past to characterize the same materials at different institutes [8, 9]. The design of the testing machines, the specimen dimensions, the test parameters, and the evaluation procedures differ. As a result, the participating testing laboratories determined not only quantitatively but also qualitatively deviating results.

In addition, there is the issue of scattering of results [10–17]. Between different repetitions of the same test, variations of up to 20% in total crack length are to be expected [16]. Therefore, a common practice for Varestraint tests is to test at least two, preferably three specimens per parameter set. A detailed analysis of possible sources of error in the measurement of crack lengths was carried out by Andersson et al. [10]. For this purpose, tests were conducted with different bending speeds, welding speeds, total strains, and welding currents. The measured standard errors were between 2 and 134% of the respective mean values of the parameter set, depending on the specimen.

Finally, the human factor in the evaluation is another uncertainty. If the same specimens are evaluated by different persons, significant deviations are to be expected [15, 16]. This is especially pronounced for small crack lengths. Digital evaluations with higher resolutions increase the number and length of cracks registered by the user.

Most of the evaluation methods used in Varestraint testing provide the number and length of cracks that form on a standardized specimen under certain test conditions. Since they do not provide any information on temperatures or

strains, they do not represent material properties. Their significance is limited to the test parameters used. Due to the numerous process-specific influencing factors, such results are only of limited suitability for comparing material-specific solidification cracking susceptibilities [18]. This applies in particular to the total crack lengths often determined in Varestraint tests. Nevertheless, there are possibilities to relate the start and end points of individual solidification cracks to the temperatures and strains according to the BTR.

## 1.2 Quantification of material-specific properties from Varestraint test results

The most direct way to do this is to determine the so-called maximum crack distance (MCD). This is the maximum crack length measured perpendicular to the melt pool isotherms [5]. The geometric range where solidification cracks can form and grow is derived from the upper and lower limit temperatures of the BTR. Since this temperature range is a material property, this theoretically also applies to the MCD. The prerequisite for this is that the deformation of the specimen is quasi-instantaneous [19]. Shankar et al. [12] report that the MCD from Varestraint tests correlate closely with the maximum crack lengths (MCL) obtained in Transvarestraint tests with the otherwise same parameters. Nevertheless, this is usually not to be observed when comparing the TCL.

As the maximum length of solidification cracks is limited by the BTR a saturation limit results with gradual increase of the strain. By exceeding this so-called saturation strain, no further crack growth occurs [5]. The crack length then covers the entire BTR. Experimental verification of this saturation limit is possible, for example in Transvarestraint tests repeated at high strain rates over different augmented strains [20, 21]. The MCD is thus a direct parameter for the material behavior.

Instantaneous deformation of specimens cannot be achieved in the practice of testing. The duration of deformation leads to a possible extension of cracks by the travel

distance of the weld pool during deformation. A certain proportion of the determined crack lengths is therefore always due to the influence of the testing process. Wolf [22] proposed a correction of the maximum crack length which takes out the influence of the deformation time. In the simple case of a center line crack, this theoretically allows the actual maximum crack distance (MCD) to be determined also from slow bending tests.

Instead from crack lengths, the susceptibility to solidification cracking can also be quantified with some effort on the basis of the BTR of a material. If the cooling curve of the weld is known, the start and end points of individual solidification cracks can be assigned to temperatures, and the actual BTR of a material can be determined from this. A procedure for identifying the BTR from Vareststraint tests was described in detail by Senda et al. [23]. Here, the cooling curve of the specimens is first determined by means of thermocouples inserted directly into the melt pool. From the starting point of the crack formation as well as the crack length, the corresponding temperature range of the solidification cracking can be derived. As a parameter, the “Critical Strain Tangent” (CST) was proposed, which corresponds to the critical strain rate according to Prokhorov [1]. Later investigations showed that the CST correlates well with practical experience regarding the weldability of different alloys [18].

Matsuda et al. finally determined the exact shape of the BTR by in situ observation of crack initiation and propagation, based on various test methods [24–27]. In recent studies by Abe et al., the basic procedure was simplified by using a two-color pyrometer to determine the temperature field near the observed cracks [28]. In any case, it is necessary to determine enough pairs of values of critical temperatures individually at different strains.

A less complex way to characterize the solidification cracking behavior of a material based on crack lengths is described by Lippold et al. [20, 21]. The procedure is based on the calculation of a characteristic temperature interval. For this purpose, the saturation crack length is first determined in Transvareststraint tests at a high bending rate. Together with the weld travel speed and the cooling rate, the so-called Solidification Cracking Temperature Range (SCTR) can be calculated. SCTR offers a simple way of comparing different materials in terms of their susceptibility to cracking. The determination of several SCTR values for different load cases allows an approximate determination of the BTR with an increased level of detail [5].

Nevertheless, at present, there is still a lack of suitable methods for deriving robust and transferable statements on the solidification cracking behavior of a material from the results of different Vareststraint test setups, which are not dependent on the test procedure and the test parameters used. The motivation for developing such an assessment option arose from results of the Vareststraint test setup (MVT)

used at BAM, which have shown dependencies from the machine parameters.

### 1.3 The significance of the crack lengths obtained from the MVT test

The evaluation of several MVT tests carried out under varying heat input as well as weld travel speeds and bending speeds led to inconsistent results regarding the influences of the individual test parameters without being able to show systematic dependencies [7]. While the discrepancies were initially assumed to be due to the material behavior, a detailed examination of the interaction between welding and loading parameters revealed that the causes were to be found in the conventional evaluation based solely on crack lengths.

The result of the conventional evaluation of the MVT specimens is the Total Crack Length TCL as the sum of the lengths of all cracks. The position of the cracks around the weld pool is not considered. While the lowest temperature gradient is present in the center of the weld, the isotherms and thus the crack critical areas are much narrower near the fusion lines. Short cracks near the fusion lines are equivalent in terms of cracking susceptibility to long cracks formed in the center of the weld metal, as they represent the same temperature range BTR in case of saturated cracking. Nevertheless, in the conventional evaluation, the same material with short off-center cracks would be rated better than with long-centered cracks. Figure 2a shows an example.

Another disadvantage of the evaluation by means of the TCL is that the cracks may grow further the longer the loading (bending deformation) continues. That is, slower deformation leads to a longer duration of the load, even if the augmented strain remains the same. The effect additionally interacts with the weld travel speed, which determines the distance over which the crack-critical zone has travelled during loading [29]. Both aspects can lead to results or apparent trends of the crack length that are difficult to interpret [7]. Another influence comes from the number of cracks. A large number of short cracks may produce the same TCL as a single long crack. However, this problem can be solved by evaluating the maximum crack length MCL.

Figure 2 b gives an example of a typical result of an MVT test. Several cracks initiate along an isotherm during loading and then grow by a certain amount with the solidification direction of the dendrites towards the center of the weld pool. On the one hand, this amount is composed of a material-specific fraction  $d_{\text{BTR}}$ , which represents the solidification crack-critical temperature interval, e.g., according to Prokhorov [1]. However, since the load required for crack initiation is not instantaneous due to the limitation of the equipment, the crack length also includes a component  $d_{\text{def}}$ , which results from the movement of the upper and lower boundary isotherms due to the travelling weld pool during

**Fig. 2** Although crack 1 is longer than crack 2 ( $L_1 > L_2$ ), both saturated crack lengths equally represent the width of the brittle temperature range BTR outlined in red and thus the solidification cracking susceptibility of the material (a); various off-center cracks as a result of an MVT test (b)

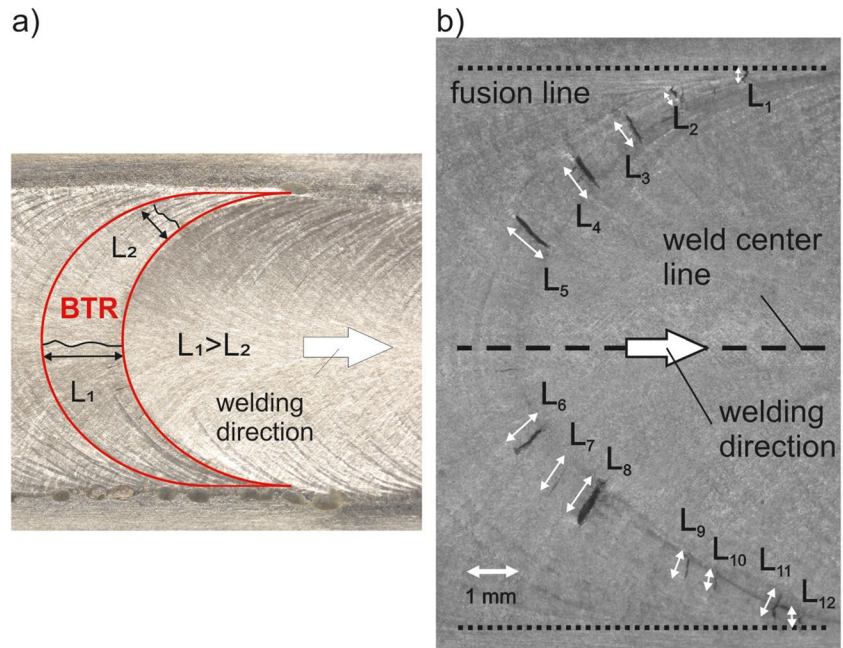


**Table 1** MVT-specific load parameters (Varestraint mode)

Parameter	Stroke distance (augmented strain)					
	0.285 mm (1%)		0.57 mm (2%)		1.14 mm (4%)	
Deformation speed/ram speed	2 mm/s	18 mm/s	2 mm/s	18 mm/s	2 mm/s	18 mm/s
Deformation time	0.143 s	0.016 s	0.285 s	0.032 s	0.57 s	0.063 s

the deformation period. The value  $d_{def}$  is called *deformation-induced crack length* in the following. The loading time is given by the stroke distance (augmented strain) and the deformation speed (ram speed). Table 1 shows typical values for the MVT test setup in the Varestraint mode.

Both components  $d_{BTR}$  and  $d_{def}$  may overlap and cannot be distinguished exactly without knowledge of the temperature distribution. In addition, it is not initially known whether a specific crack is saturated, meaning that it actually represents the entire BTR of the material. In the simplest case of a saturated weld center crack, the crack portion  $d_{def}$  corresponds 1:1 to the weld pool travel distance during deformation, see Eq. 1.

$$d_{def,centerline} = v_t \cdot t_{def} \tag{1}$$

with:

- $v_t$ —weld travel speed
- $t_{def}$ —deformation time

However, this linear relationship does not apply to off-center cracks. In an idealized way, these cracks follow rather a curved path, which is determined by the direction of solidification, i.e., the temperature gradient. Figure 3 shows a schematic. If the ideal crack growth paths/

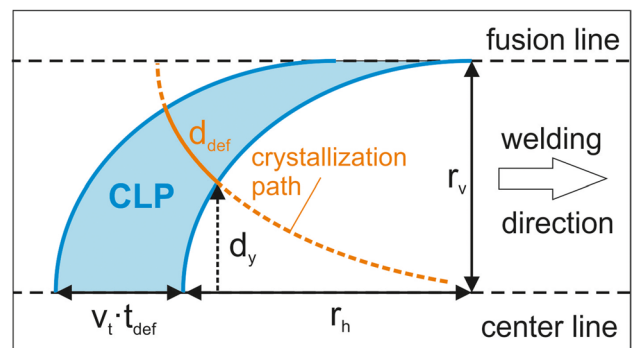


**Fig. 3** Deformation-induced crack length  $d_{def}$  along the crystallization path during deformation at the distance  $d_y$  from the weld centerline;  $v_t$ , weld travel speed;  $t_{def}$ , deformation time;  $r_h$ , horizontal weld radius;  $r_v$ , vertical weld radius. The integral of all  $d_{def}$  is the crack length potential CLP

crystallization directions can be calculated,  $d_{def}$  can be determined for any position behind the weld pool [30]. The area which is crossed by an isotherm during the deformation is the integral of all  $d_{def}$  and is called CLP (crack length potential) in the following. While the BTR describes a temperature interval, the integral CLP represents its shift while the deformation.

With knowledge of the deformation induced length of a crack  $d_{\text{def}}$ , a relative crack length  $rcl$  can now be formulated, which compares the actually occurring crack length  $L$  with  $d_{\text{def}}$ , Eq. 2. The value  $rcl$  is calculated regardless of whether the crack is saturated or not. If several cracks occur in a sample, the arithmetic mean RCL of all relative crack lengths of the individual cracks is determined and taken as the characteristic value for the sample. Future evaluations will show whether this assumption is practicable in all cases. As an alternative to the average RCL of all individual cracks in a sample, the relative crack length can be determined for the longest individual crack (MCL).

$$rcl = \frac{L}{d_{\text{def}}} \quad (2)$$

$$RCL = \frac{\sum rcl}{n} \quad (3)$$

with:

$L$ —crack length (composed of unknown portions of  $d_{\text{BTR}}$  and  $d_{\text{def}}$ )

$n$ —number of cracks

For RCL three cases can be distinguished as follows:

Case 1:  $RCL = 0$  (i.e.,  $L = 0$ )

No cracking occurs.

Case 2:  $0 < RCL < 1$  (i.e.,  $L < d_{\text{def}}$ )

The average crack length measured is shorter than the distance which the isotherms have travelled while loading. The cracking susceptibility is rather low or the cracks are not saturated. For results in this category, an influence of the machine parameters on the crack lengths cannot be excluded. Tests with higher loads and loading speeds or shorter deformation times are recommended.

Case 3:  $RCL \geq 1$  (i.e.,  $L \geq d_{\text{def}}$ )

The average crack length is at least equivalent to the load duration. With  $RCL > 2$ , the material factor  $d_{\text{BTR}}$  becomes greater than the machine factor  $d_{\text{def}}$ . Here, it can be assumed that the determined crack length is only slightly influenced by the load duration and the cracks are probably saturated.

Nevertheless, the evaluation according to RCL cannot prove whether a crack is saturated. Even with saturated cracks, RCL can be small if the saturation crack length is small and in the range of  $d_{\text{def}}$ . Higher loading speeds are then recommended in order to keep  $d_{\text{def}}$  as small as possible.

It should be emphasized at this point that the result of this work does not represent a new crack criterion per se and does not call existing solidification crack theories into question. Rather, a tool is provided which describes the solidification cracking behavior of a material in relation to the testing and welding parameters used. This allows an evaluation of how strongly the test parameters affect the test result total crack length (TCL).

The subsequent section first describes, on the basis of a numerical parameter study, how the isolated variation of individual welding and loading parameters affects the deformation-induced crack lengths  $d_{\text{def}}$  within the parameter range of the MVT test. Experimental results of the classical and new evaluation are compared and discussed then. A total of 2598 solidification cracks on 117 specimens were evaluated. For this purpose, an image-based digital crack selection routine was developed which is described exemplarily.

## 2 Sensitivity analysis on the influence of the MVT test parameters on the deformation-induced crack length

Although the literature attributes a decisive role to the parameters used in the Vrestraint test [15, 24, 31–34], there are currently no complete, systematic analyses of the influence of individual test parameters on the results, especially for the MVT test variant used at BAM. In particular, the standard deformation speed (ram speed) of the MVT test is specified as rather low, compare Table 1. The influence of the boundary conditions is therefore estimated in the following by numerical calculations. In contrast to reality, individual parameters can be varied and isolated from each other. This involves the parameters horizontal weld pool radius  $r_h$ , vertical weld pool radius  $r_v$ , and weld travel speed  $v_t$ , see Fig. 3.

The target value of the calculations is the value  $d_{\text{def}}$ , which quantifies the elongation of the crack-susceptible zone by the moving weld pool during loading (deformation-induced crack length). The individual position along the weld pool ellipse is considered, i.e., the crack growth occurs along the assumed crystallization paths, see also Fig. 3. A vertical weld pool radius  $r_h$  of 4 mm, a horizontal weld pool radius  $r_h$  of 5 mm, a weld travel speed  $v_t$  of 3 mm/s, and a deformation speed  $t_{\text{def}}$  of 2 mm/s were used as the central point of the comparisons. The above parameters were varied individually within the limits given in Table 2 and are based on the values typically encountered in MVT testing. A total of 15,730 parameter combinations were evaluated.

In the following plots,  $d_{\text{def}}$  is given as a function of the distance  $d_y$  (see Fig. 3). For  $d_y = 0$  (weld centerline),  $d_{\text{def}}$

**Table 2** Parameter variation for assessment of the deformation-induced crack length  $d_{\text{def}}$

Parameter	Variation	Central point
Vertical weld pool radius $r_v$	3–5 mm	4 mm
Horizontal weld pool radius $r_h$	3–7 mm	5 mm
Weld travel speed $v_t$	1.8–3.6 mm/s	3 mm/s
Deformation speed $v_{\text{def}}$	2–18 mm/s	2 mm/s

is always at its maximum (weld centerline crack). With increasing  $d_y$ ,  $d_{\text{def}}$  decreases and approaches 0 at the fusion line.

Higher weld widths ( $r_v$ , Fig. 4a) increase the potential crack lengths due to the expanding weld pool. It may be surprising that a change in the horizontal weld pool radius (Fig. 4b)—i.e., a tension or compression of the weld pool in the welding direction—does not lead to a change of  $d_{\text{def}}$  in the center of the weld. This is because, in contrast to reality, the welding speed remains constant in the calculation and the weld pool travels the same distance (= center line crack length) in every case. However, smaller radii  $r_h$  lead to a compression of the weld pool ellipse, which results in longer crystallization paths away from the weld center. As a result, the potential crack length increases somewhat there. The sole increase in weld travel speed (Fig. 4c) shows an increase in the maximum possible crack length at all positions along the weld pool ellipse. In the center of the weld, there is a direct proportionality. A doubling of the weld travel speed, according to Eq. 1, also doubles  $d_{\text{def}}$ .

The same linear dependence is present for the deformation speed. Here, however, the effects shown in Fig. 4d are more pronounced since the deformation speed was varied within wider limits (factor 9) than the weld travel speed (factor 2). This corresponds to the actual parameter window of the MVT test, which means that the effects of variable deformation speeds are expected to have by far the largest impact on crack lengths. In this context, low deformation speeds in combination with high weld travel speeds predict the strongest influence of the test sequence on the extent of crack formation.

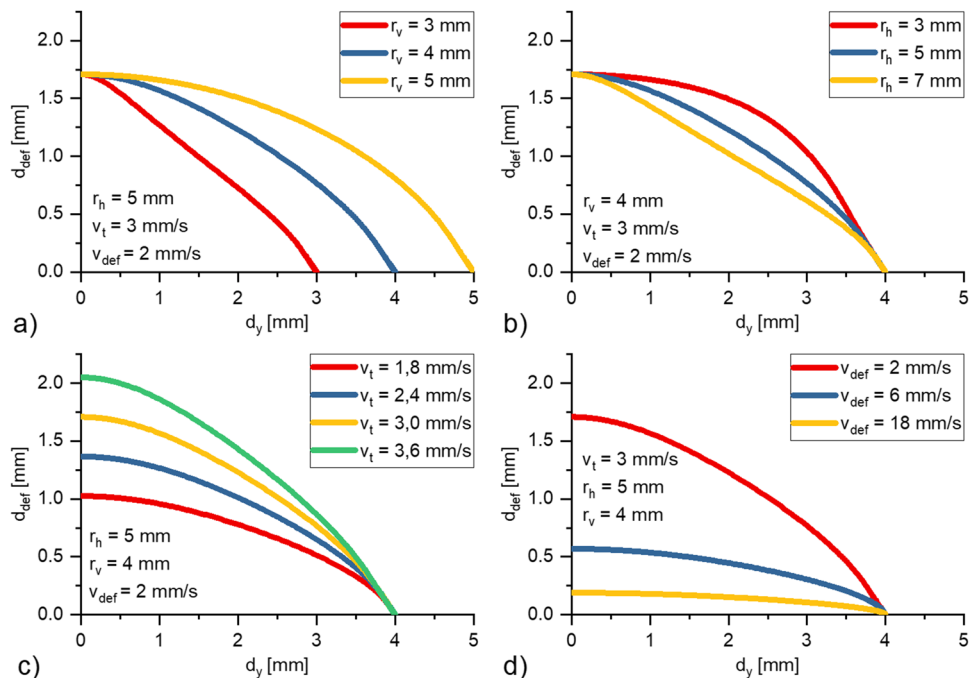
The area integrals covered by the individual  $d_{\text{def}}$  curves in Fig. 3 correspond to the area of the material-independent, i.e., machine-specific, movement of the isotherms during deformation. Thus, they characterize the potential of the maximum possible crack propagation for the given process parameters. The area integrals of the  $d_{\text{def}}$  curves are therefore considered in the following as the crack length potential *CLP*, see Fig. 3. Different parameter sets can be evaluated this way.

Figure 5 contains three individual diagrams showing the *CLP* as a function of the deformation speed. They quantify the interactions with the three other parameters by means of the additional color scales. Each of them thus shows the value of the *CLP* as a function of two parameters, while the two remaining parameters are fixed. Their values are noted at the top of the diagram.

A higher deformation speed leads to reaching the complete deformation (augmented strain) in a shorter period of time. Thus, the *CLP* decreases with increasing deformation speed. The exponential character (hyperbola), which may be surprising at first glance, is explained by the fact that the deformation time is inversely proportional to the deformation rate as described by Eq. 1. The lowest machine-specific influence on the crack length is to be expected for the fastest possible deformation. This is consistent with previous recommendations [5]. Above a value of approx. 10 mm/s, the influence of varying deformation speeds on the crack length potential is within the range of the other factors investigated.

The influence of the weld travel speed and the weld pool radii is much smaller, which can be seen from the respective spread of the curve arrays. In addition, an increasing

**Fig. 4** Deformation-induced crack length  $d_{\text{def}}$  as a function of the distance from the weld center  $d_y$  with variation of the vertical weld pool radius  $r_v$  (a), the horizontal weld pool radius  $r_h$  (b), the weld travel speed  $v_t$  (c), and the deformation speed  $v_{\text{def}}$  (d). See also Fig. 3



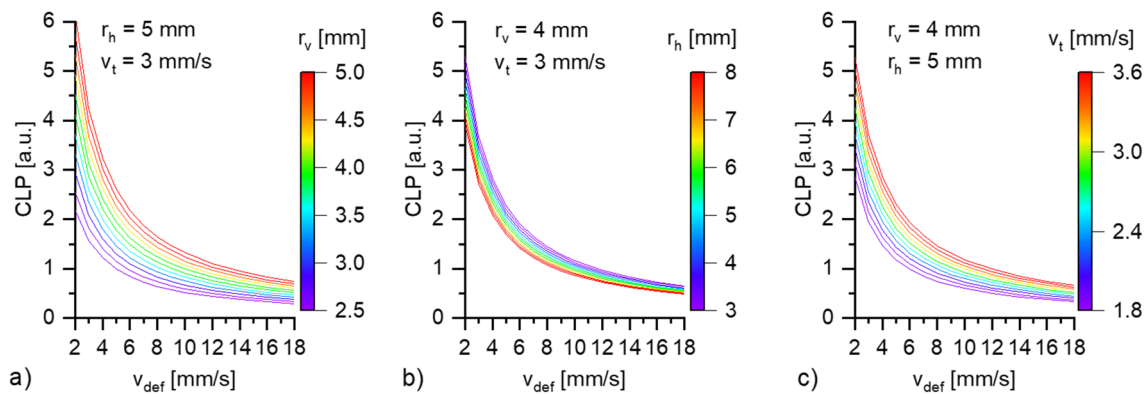


**Fig. 5** Influence of different test parameters on the crack length potential CLP, plotted as a function of the deformation speed  $v_{\text{def}}$ . Vertical weld pool radius (a), horizontal weld pool radius (b), and weld travel speed (c)

weld travel speed is associated in reality with an increase in the horizontal and a simultaneous decrease in the vertical weld pool radius. Both counteract the effect of the weld travel speed on the CLP. Therefore, it can be assumed that changes in the weld travel speed within the parameter range considered are not expected to have any significant influence on the deformation-induced crack growth.

To be able to take the influences shown into account in the MVT evaluation, i.e., calculation of the relative crack length  $RCL$  following Eqs. 2 and 3, all cracks that have occurred as well as the weld pool geometry must be quantified. For this purpose, a MATLAB [35]-based evaluation routine was programmed. Its application is briefly illustrated by an example in the following. The program code was developed and published by Maximilian Thomas [36].

### 3 Digital evaluation routine for quantification of cracks and weld pool characteristics

The evaluation routine is initially divided into the steps of crack selection and selection of the weld pool parameters. These two steps need input from the user. Once this has been completed, the results are calculated. The application of the software requires at least one high-resolution surface image of the specimen with a known image scale. In present case, images with a resolution of  $5184 \times 3888$  pixels were used. The image scale was 301.35 pixels/mm.

#### 3.1 Crack selection

At least one surface image in JPG format is selected first. The images should show a horizontal orientation of the weld seam running from left to right. The optional selection of up to three images under different exposure angles can support

the subsequent crack selection. The following metadata must be entered for each sample before starting the evaluation:

- Specimen ID
- Weld travel speed (mm/s)
- Deformation speed (mm/s)
- Augmented strain (%)
- Type of test (Varestraint or Transvarestraint)
- Specimen thickness (mm)
- Specimen width (mm)

Besides the identifier, the inputs are required for the calculation of the deformation time  $t_{\text{def}}$ .

All cracks found on the surface of the specimen are selected using point and click. Each single connected green area is later treated as a single crack. Figure 6a shows an example of selected cracks in the program window and the current magnification factor. The cracks can be selected in two ways.

Using “Region Growing,” the crack is defined based on a gray value comparison. After selecting a pixel by mouse click, an iterative comparison with the surrounding pixels takes place, based on the respective gray values. The sensitivity is adjusted individually by means of a threshold value. Some cracks may be too narrow or not sufficiently monochrome that they can be selected using the region-growing algorithm. In these cases, the course of the crack can be traced point by point along individual straight lines.

#### 3.2 Selection of the weld pool parameters

In this step, the weld geometry is specified. First, the position of the fusion lines, which appear as dashed lines, is defined. In addition, the weld centerline is also displayed as a dashed line. Furthermore, two half-ellipses are created, which indicate the shape of the weld pool. Their positioning is based on the weld contour. Ripple lines are helpful here.

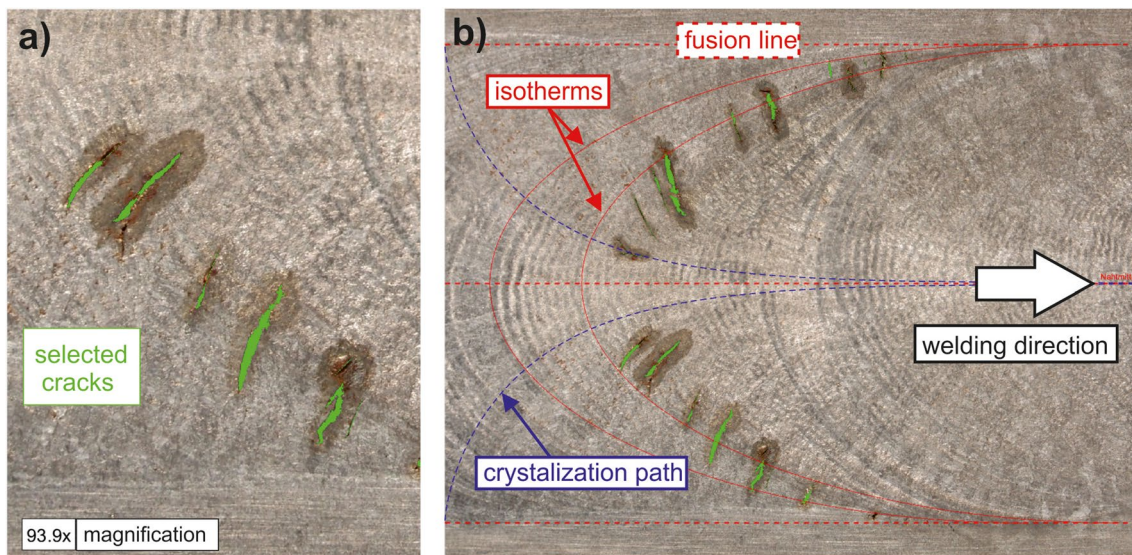


**Fig. 6** Exemplary crack selection (a) and weld geometry selection (b); selected cracks in green; exemplary isotherms in red (solid line); exemplary crystallization paths in blue

The horizontal radius can thus be adjusted individually. The vertical ellipse radius is already specified by the weld width (fusion lines). Figure 6b shows an example. The theoretical crystallization direction is also shown by means of blue dashed lines. The distance between the two red ellipses in the weld center corresponds to the torch travel distance during deformation (Eq. 1). Note that for the calculations the simplification is made that the selected weld pool boundary ellipses correspond to the individual isotherms in the mushy zone.

### 3.3 Crack analysis

After all cracks as well as the weld pool characteristics have been selected, several properties are calculated for each crack using the MATLAB [35] function “RegionProps.” These include, among others, the main parameters:

1. Crack length  $L$  (mm): longest distance within a contiguous selected region.
2. Total crack length  $TCL$  (mm): sum of all crack lengths  $L$ .
3. Deformation-induced crack length  $d_{\text{def}}$  (mm): The maximum fraction of a crack length  $L$  that is attributed to the duration of deformation. For its calculation, it is assumed that the crack under consideration grows following the crystallization path over the entire period of deformation (but not beyond).  $d_{\text{def}}$  thus describes the portion of a crack due to the machine specifics whose propagation is not stopped during deformation. See also Figs. 3 and 4.

4. Relative crack length  $rcl$  (%): Ratio of actual crack length  $L$  to the maximum deformation-induced crack length component  $d_{\text{def}}$  (see Eq. 2).
5. Average relative crack length  $RCL$  (%): arithmetic mean of all relative crack lengths (see Eq. 3).

Some of these properties require the individual crystallization paths for the cracks selected. The paths are calculated numerically from the fusion line to the center of the weld from the previously defined elliptical weld pool shape. The algorithm used is based on the horizontal displacement of normals, which are applied in constant steps to the course of the weld pool front. The numerical implementation is described in detail in [30, 37].

In principle, the software can also be applied to results (samples) from other Varestraint setups. The deformation times required to achieve certain strains are required. This data would have to be implemented in the program code once by the user. Only a high-resolution surface image of the sample is then required for evaluation.

## 4 Examples

### 4.1 Experimental

Three different materials tested under varying parameter sets are shown in the following, applying the classical ( $TCL$ ) as well as the evaluation based on the relative crack length  $RCL$ . All samples were evaluated by the software tool described before. The materials were chosen because of their specific solidification cracking response in the MVT

test. The metallurgical reasons for cracking are discussed elsewhere [37, 38]. Each chemical composition is given in Table 3. While alloy A is the Ni-based alloy 602 CA (2.4633), alloys B and C are non-commercial martensitic welding consumables.

The welding parameters were varied following Table 4, which is the typical range in MVT testing. The loading parameters are also shown in Table 4. The stroke rate (ram speed) was varied by a factor of nine up to the maximum of the setup. The correspondent deformation time is also included in the table and used subsequently for the presentation of the results. Vareststraint mode was applied in most cases. Some tests of alloys B and C were conducted in Transvareststraint mode. Three repetitions were made for each parameter set.

## 4.2 Results

Figure 7a to c show the results of the evaluation according to the total crack length *TCL* for the individual parameter sets as a function of the deformation time. For rapid bending respectively short deformation times, the crack lengths are close to each other. While alloy A (Fig. 7a) gives the longest cracks, alloys B (Fig. 7b) and C (Fig. 7c) allow no clear ranking. In tendency, alloy B shows slightly longer cracks. With increasing deformation time, the differences between the alloys become higher. While the crack length of alloy A increases nearly, linear alloys B and C remain constant or even show decreasing crack lengths. This is an unexpected behavior which has its origin in the influence in the MVT test characteristics.

In Fig. 7d to f, the relative crack length *RCL* is plotted as a function of the deformation time separated for each alloy. The values decrease for all materials and parameter sets for longer deformation times. In particular, alloy A shows a strong dependence of the value *RCL* on the deformation time. Even though the number of data points is small, the hyperbolic character already predicted in the numerical analysis (cf. Figure 5) is visible here. That means that the high *TCL*s found for long deformation times are a consequence of higher  $d_{\text{def}}$  values and therefore artifacts. In contrast to the *TCL*, the *RCL* values approach each other below  $RCL = 1$  for longer deformation times. Remember that a small  $RCL < 1$  indicates a major influence of the machine characteristics on the crack length.

**Table 3** Chemical compositions in wt.%

Alloy	C	Cr	Ni	Mn	Si	Cu	Al	Ti	Fe
A	0.2	25.5	Bal	0.04	0.02	0.01	2.32	0.17	8.91
B	0.07	7.4	6.1	0.5	0.27	-	-	-	Bal
C	0.07	10.3	0.04	9.5	0.38	-	-	-	Bal

**Table 4** Welding and loading parameters applied in MVT test

Parameter	Range
Heat input per unit length (kJ/cm)	7.6–14
Weld travel speed (mm/s)	1.8–3.6
Augmented strain (%)	2–4
Stroke rate (mm/s)	2–18
Deformation time (s)*	0.032–0.57 (Vareststraint) 0.068–0.62 (Transvareststraint)

\*Differences in deformation time between Vareststraint and Transvareststraint are due to different designs of the bending dies

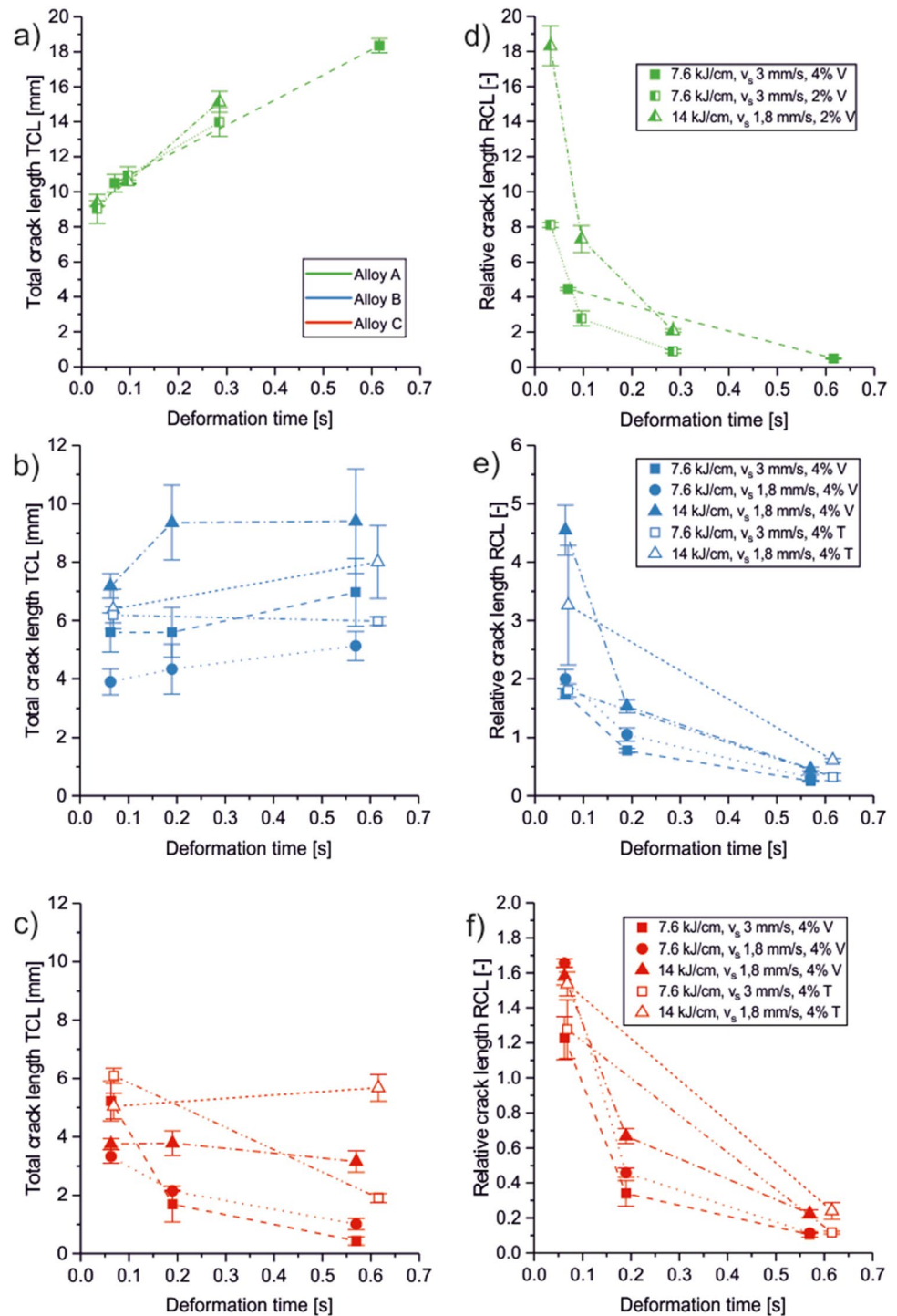
The ranking of the materials, i.e., the evaluation of the cracking susceptibility, is in most cases similar as observed for *TCL*. Nevertheless, individual parameter sets differ in their effect when comparing *TCL* and *RCL*. For alloy A, the *TCL* is very similar for the three welding parameter sets used whereas *RCL* is significantly different. *RCL* therefore may allow for a separation or more detailed ranking of individual parameter sets if necessary. On the other hand, a small spread of *RCL* for a single material reveals a minor influence of the welding parameters, even if *TCL* indicates erroneously an opposite behavior as in case of alloy C.

For a better separation of the individual curves, Fig. 8a shows a logarithmic representation of the relative crack length *RCL* as a function of the deformation time. Most of the curves are parallel and appear linear on the logarithmic scale. Against the background of the three cases of *RCL* evaluation described in Sect. 1.3, alloy C exceeds the value 1 only at the shortest deformation time. At longer deformation times, the cracks are shorter than the load duration would suggest. Alloy A is mostly above  $RCL = 1$  which indicates a minor influence of the loading duration on the crack growth in these cases. The deformation-induced crack length is very small in comparison. Alloy B ranks between the other two alloys.

For the assessment of the susceptibility to cracking, this means that for results with  $RCL < 1$ , it is recommended to aim for further tests with higher deformation rates or shorter deformation times to minimize  $d_{\text{def}}$ .

For clarification, it should be mentioned again that an increase in the relative crack length is not generally to be regarded as equivalent to an increase in the cracking susceptibility of the material. Rather, the relative crack length documents how strongly the cracking behavior may be

**Fig. 7** Total crack length TCL of alloys A (a), B (b), and C (c) and relative crack length RCL of alloys A (d), B (e), and C (f) as a function of the deformation time applied (parameters heat input, weld travel speed, augmented strain, and  $\bar{\nu}$  are indicated in the legend)



influenced by the MVT parameters. Nevertheless, RCL can also be used to compare the absolute solidification cracking susceptibility of several materials—if an identical MVT parameter range was applied. This is illustrated in the following.

Here, the linear characteristic of RCL versus the deformation time on the logarithmic scale is utilized. To quantify a characteristic single value for a set of welding parameters,

the intersection of the individual straight lines with  $RCL = 1$  is determined (dashed line, see Fig. 8a). The resulting values are given in Fig. 8b) for all parameter sets applied. The higher the value of this “critical” deformation time  $t_{def,1}$ , the higher the solidification cracking susceptibility of the material is to be estimated under the given boundary conditions.

Slower welding produces higher RCL values for each alloy. The same is indicated with increasing heat input.

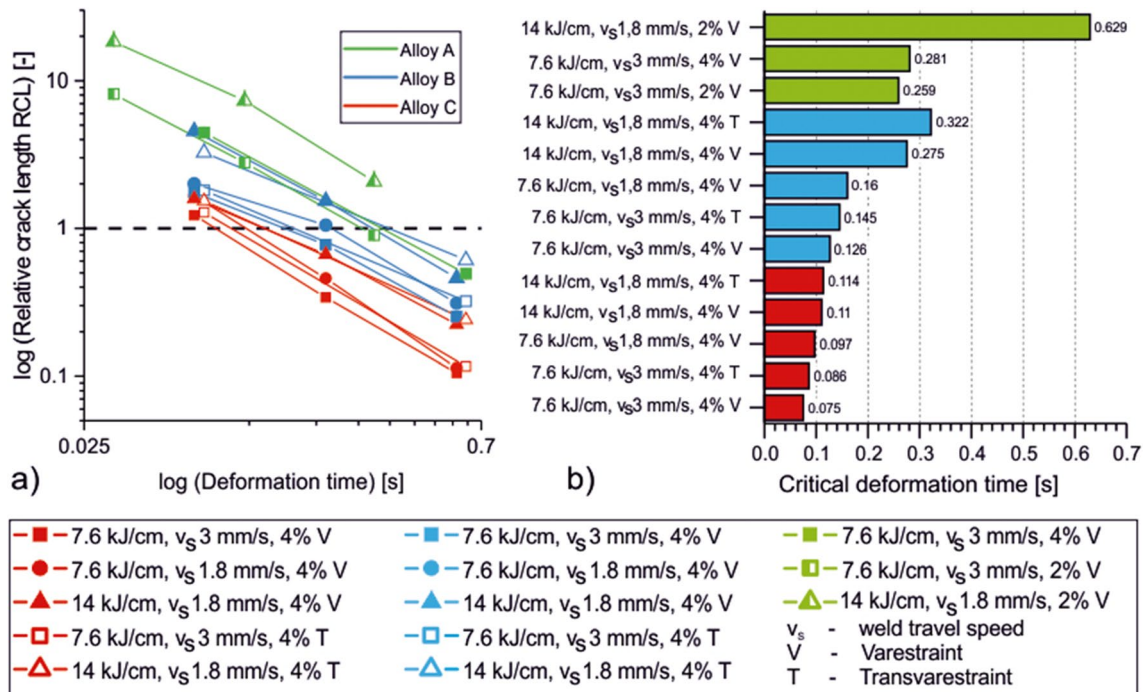


**Fig. 8** Relative crack length RCL (log) as a function of the deformation time applied (a) and critical deformation time  $d_{def,1}$  calculated for all parameter sets (b)

Varestraint and Transvarestraint variants of the same parameter set are close to each other. Nevertheless, each Transvarestraint variant shows a slightly higher value compared to the Varestraint variant. The reason may stem from the differing mechanical setup (design of the bending dies) and therefore slightly different deformation times for reaching the same augmented strain, see Table 4 and also Fig. 7.

All these dependencies cannot be derived from the total crack length TCL, cf. Figure 7a to c. In an earlier study, an evaluation of some of the samples considered here was examined with regard to the influence of the strain rate [30]. It was shown that this also allows a ranking of individual parameter sets, but only meaningful with the same total strain. The dependence on the deformation time presented here, on the other hand, can take variable total strains into account.

By taking several deformation times into account, it is also possible to compare the results of different Varestraint setups from other laboratories. The crack lengths determined cannot yet be compared directly. However, it is possible to assess the extent to which the crack lengths may be affected by the loading parameters. Round robin tests involving different laboratories are to be aimed for in the future.

### 5 Summary and conclusions

An image-based digital crack detection routine was developed to include the effect of crack orientation as well as load duration in the evaluation of Varestraint and Transvarestraint test results. Based on the weld pool characteristics, the shape of the isotherms is reconstructed, and the theoretical crack growth along numerically determined crystallization paths is considered in relation to the cracks that actually occur. The index *relative crack length* RCL derived from this allows an extended assessment of the material behavior during the test. The threshold introduced can quantify the dependencies of the crack formation from the welding and testing parameters, which could not be comprehensively identified with the conventional evaluation. The relative crack length is not an index describing the cracking susceptibility—it is rather an additional measure helping to evaluate the machine influence on the crack length obtained from Varestraint tests under varying boundary conditions. It can help to identify unsuitable test parameters. In principle, the evaluation routine can also be transferred to other Varestraint or even other externally loaded hot cracking tests allowing a comparison of the crack lengths obtained. A sensitivity analysis of typical

welding and loading parameters applied in the Modified Vareststraint Transvareststraint test setup revealed that the deformation rate is the major factor on the potential crack length. Variations in the welding parameters have a minor influence. To minimize the influence of machine and welding parameters, high strain rates combined with slow welding speeds are recommended.

**Acknowledgements** This research was funded by the German Research Foundation (DFG), grant numbers KR3917/2-2, KA1807/9-1, and GI376/8-1.

**Funding** Open Access funding enabled and organized by Projekt DEAL.

**Data availability** The raw data is not accessible by the public but can be made available on demand by the corresponding author.

## Declarations

**Competing interests** The authors declare no competing interests.

**Open Access** This article is licensed under a Creative Commons Attribution 4.0 International License, which permits use, sharing, adaptation, distribution and reproduction in any medium or format, as long as you give appropriate credit to the original author(s) and the source, provide a link to the Creative Commons licence, and indicate if changes were made. The images or other third party material in this article are included in the article's Creative Commons licence, unless indicated otherwise in a credit line to the material. If material is not included in the article's Creative Commons licence and your intended use is not permitted by statutory regulation or exceeds the permitted use, you will need to obtain permission directly from the copyright holder. To view a copy of this licence, visit <http://creativecommons.org/licenses/by/4.0/>.

## References

1. Prokhorov NN, Prokhorov NN (1971) Fundamentals of the theory for technological of metals while crystallising during welding. *Trans Jpn Weld Soc* 2:109–117
2. Kannengiesser T, Boellinghaus T (2014) Hot cracking tests—an overview of present technologies and applications. *Weld World* 58:397–421. <https://doi.org/10.1007/s40194-014-0126-y>
3. Wilken K, Kleistner H (1982) Der MVT-Test - ein neues universelles Verfahren zur Prüfung der Heissrissanfälligkeit beim Schweißen. *Mater Technik* 1:3–10 (in German)
4. Savage WF, Lundin CD (1965) The Vareststraint test. *Weld J Res Suppl* 10:433–470
5. Lippold JC (2015) *Welding metallurgy and weldability*. John Wiley & Sons Inc, Hoboken, New Jersey
6. Coniglio N, Cross C (2016) Towards establishment of weldability testing standards for solidification cracking. In: Boellinghaus T, Lippold JC, Cross CE (eds) *Cracking phenomena in welds IV*. Springer International Publishing, Switzerland, pp 37–66
7. Thomas M et al (2020) Surface- and volume-based investigation on influences of different Vareststraint testing parameters and chemical compositions on solidification cracking in LTT filler metals. *Weld World* 64:913–923. <https://doi.org/10.1007/s40194-020-00895-2>
8. Wilken K (1999) Investigation to compare hot cracking tests - externally loaded specimens. International Institute of Welding, IIW Doc. IX-1945–99
9. Finton T, Lippold JC, Bowers R (1999): Comparison of weld hot cracking tests, summary of an IIW round robin study, IIW Doc. IX-H-459–99 (II-C-175–99)
10. Andersson J, Jacobsson J, Lundin C (2016) A historical perspective on Vareststraint testing and the importance of testing parameters. In: Boellinghaus T, Lippold JC Cross CE (eds) *Cracking phenomena in welds IV*. Springer International Publishing, Switzerland, pp 3–23
11. Singh S, Andersson J (2018) Hot cracking in cast alloy 718. *Sci Technol Weld Join* 23:568–574. <https://doi.org/10.1080/13621718.2018.1429238>
12. Shankar V, Gill TPS, Mannan SL, Sundaresan S (2013) Criteria for hot cracking evaluation in austenitic stainless steel welds using longitudinal vareststraint and transvareststraint tests. *Sci Technol Weld Join* 5:91–97. <https://doi.org/10.1179/136217100101538074>
13. Shankar V, Gill TPS, Mannan SL, Sundaresan S (2003) Solidification cracking in austenitic stainless steel welds. *Sadhana* 28:359–382. <https://doi.org/10.1007/bf02706438>
14. Singh S, Andersson J (2018) Vareststraint weldability testing of cast ATI® 718Plus™—a comparison to cast Alloy 718. *Weld World* 63:389–399. <https://doi.org/10.1007/s40194-018-0626-2>
15. Johansson MM, Stenvall P, Karlsson L, Andersson J (2020) Evaluation of test results and ranking criteria for Vareststraint testing of an austenitic high-temperature alloy. *Weld World* 64:903–912. <https://doi.org/10.1007/s40194-020-00891-6>
16. Lingenfelter A (1972) Vareststraint Testing of Nickel Alloys. *Weld J* 51:430–436
17. Savage W, Lundin C (1966) Application of the Vareststraint technique to the study of weldability. *Weld J* 45:497–503
18. Coniglio N, Cross C (2013) Initiation and growth mechanisms for weld solidification cracking. *Int Mater Rev* 58:375–397. <https://doi.org/10.1179/1743280413y.0000000020>
19. Robino CVR, Reece M, Knorovsky GA, DuPont J, Feng Z (2006) Prediction of maximum crack length in longitudinal vareststraint testing. In: David SA, DeRoy T, Lippold JC, Smartt HB, Vitek KM (eds) *Trends in welding research: Proceedings of the 7th International Conference*. ASM International, Material Park, Ohio pp 313–318
20. Lippold JC, Lin WM (1996) Weldability of commercial Al-Cu-Li alloys. *Mater Sci Forum* 217–222:1685–1690. <https://doi.org/10.4028/www.scientific.net/MSF.217-222.1685>
21. Lippold JC (2005) Recent developments in weldability testing. In: Boellinghaus T, Herold H (eds) *Hot Cracking Phenomena in Welds*. Springer, Berlin, Heidelberg, New York, pp 271–290
22. Wolf M (2006) Zur Phänomenologie der Heißrissbildung beim Schweißen und Entwicklung aussagekräftiger Prüfverfahren, in BAM Bundesanstalt für Materialforschung und -prüfung BAM-Dissertationsreihe Band 19, Helmut-Schmidt-Universität/Universität der Bundeswehr Hamburg: Berlin, p 218 (in German)
23. Senda T et al (1971) Fundamental Investigations on solidification crack susceptibility for weld metals with trans-vareststraint Test. *Trans Jpn Weld Soc* 2:45–66
24. Matsuda F, Nakagawa H, Nakata K, Kohmoto H, Honda Y (1983) Quantitative evaluation of solidification brittleness of weld metal during solidification by means of in-situ observation and measurement (report I): development of the MISO technique. *Trans JWRI* 12:65–72
25. Matsuda F, Nakagawa H, Kohmoto H, Honda Y, Matsubara Y (1983) Quantitative evaluation of solidification brittleness of weld metal during solidification by means of in-situ observation and measurement (report II): solidification ductility curves for steels with the MISO technique. *Trans JWRI* 12:73–80

26. Matsuda F, Nakagawa H, Tomita S (1986) Quantitative evaluation of solidification brittleness of weld metal during solidification by in-situ observation and measurement (report III): effect of strain rate on minimum ductility required for solidification crack initiation in carbon steels, stainless steels and inconel Alloy. *Trans JWRI* 15:125–133
27. Matsuda F, Nakagawa H, Tomita S (1987) Quantitative evaluation of solidification brittleness of weld metal during solidification by in-situ observation and measurement (report IV): effect of grain-boundary sliding on strain-rate dependence of critical strain required for solidification crack initiation. *Trans JWRI* 16:317–223
28. Abe D, Matsuzaka F, Murakami Y, Matsuoka T, Yamaoka H (2018) Determining the BTR by conducting a Trans-Varestraint test using a high-speed camera and two-color pyrometry. *Weld World* 62:1237–1246. <https://doi.org/10.1007/s40194-018-0608-4>
29. Coniglio N, Cross CE (2020) Effect of weld travel speed on solidification cracking behavior. Part 1: weld metal characteristics. *Int J Adv Manuf Technol* 107:5011–5023. <https://doi.org/10.1007/s00170-020-05231-y>
30. Kromm A, Thomas M, Kannengiesser T, Gibmeier J, Vollert F (2022) Assessment of the solidification cracking susceptibility of welding consumables in the Varestraint test by means of an extended evaluation methodology. *Adv Eng Mater* 24. <https://doi.org/10.1002/adem.202101650>
31. Coniglio N, Cross CE (2020) Effect of weld travel speed on solidification cracking behavior. Part 2: testing conditions and metrics. *Int J Adv Manuf Technol* 107:5025–5038. <https://doi.org/10.1007/s00170-020-05232-x>
32. Da Silva CLM, Scotti A (2004) Performance assessment of the (Trans)Varestraint tests for determining solidification cracking susceptibility when using welding processes with filler metal. *Meas Sci Technol* 15:2215–2223. <https://doi.org/10.1088/0957-0233/15/11/006>
33. Statharas D et al (2019) Getting the strain under control: transvarestraint tests for hot cracking susceptibility. *Metall Mater Trans A Phys Metall Mater Sci* 50:1748–1762. <https://doi.org/10.1007/s11661-019-05140->
34. Yamashita S et al (2021) Quantitative evaluation of augmented strain at the weld metal during the Trans-Varestraint test. *Weld World* 65:2013–2021. <https://doi.org/10.1007/s40194-021-01152-w>
35. The MathWorks Inc (2020) MATLAB version: 9.9.0 (R2020b), Natick, Massachusetts: The MathWorks Inc. <https://www.mathworks.com>
36. Thomas M (2021) Varestraint evaluation routine. Version 1:3. <https://doi.org/10.5281/zenodo.5714473>
37. Thomas M (2022) Verbesserung der Übertragbarkeit von Erstarrungsrisssprüfungen nach dem MVT-Verfahren durch Digitalisierung der Probenauswertung, BAM Bundesanstalt für Materialforschung und -prüfung, BAM Dissertationsreihe, vol 171. Otto-von-Guericke-Universität Magdeburg, Berlin (**in German**)
38. Wolf M, Schobbert H, Boellinghaus T (2005) Influence of the weld pool geometry on solidification crack formation. In: Boellinghaus T, Herold H (eds) *Hot cracking phenomena in welds*. Springer, Berlin, Heidelberg, New York, pp 245–268

**Publisher's Note** Springer Nature remains neutral with regard to jurisdictional claims in published maps and institutional affiliations.